JOURNAL OF Applied Polymer SCIENCE

Characterization of Shear Stress at the Tool-Part Interface During Autoclave Processing of Prepreg Composites

Ronald Joven, Behrouz Tavakol, Alejandro Rodriguez, Mauricio Guzman, Bob Minaie
Department of Mechanical Engineering, Wichita State University, Wichita, Kansas 67260
Correspondence to: B. Minaie (E-mail: bob.minaie@wichita.edu)

ABSTRACT: In this article, shear stress between an aluminum tool and a carbon fiber-epoxy prepreg is characterized during cure using polymeric release agent and release film at the tool-part interface. The effects of surface roughness, release materials, pull-out speed, temperature, and normal force (autoclave pressure) on the shear stress are investigated using a customized friction rig. Results show that the interfacial shear stress decreases as the temperature increases and it increases as the normal force increases when using either the release film or the release agent. Additionally, changes in surface roughness from 1.35 to 0.18 μm decrease the shear stress 10–27% while the use of release agent shows a decrease between 23% and 51% in the shear stress. Furthermore, strong adhesion between the tool and the part is observed when using release agent and pull-out speeds of 0.05 mm/min (static/dynamic friction ratio of 5.29 $\pm$ 0.19). Using the experimental data, a mathematical approach based on the Coulomb's friction model is proposed to predict the friction force at the tool-part interface. © 2013 Wiley Periodicals, Inc. J. Appl. Polym. Sci. 129: 2017–2028, 2013

KEYWORDS: composites; thermosets; manufacturing; friction; wear and lubrication

Received 15 June 2012; accepted 6 December 2012; published online 3 January 2013
DOI: 10.1002/app.38909

INTRODUCTION

Manufacturing of large scale and complex-shaped composite structures for aerospace applications requires a precise control over the part geometrical dimensions. Strict dimensional tolerances are crucial because errors during manufacturing of thermoset composites are not easily reversible. In this context, manufacturing of these composites has been challenging due to part distortion resulting from different deformation mechanisms and frictional interactions between tool and part (Figure 1). Deformation mechanisms are normally caused by resin cure shrinkage,[1] different coefficients of thermal expansion (CTE) within ply and CTE mismatch between the tool and the part,[2] while frictional interactions are developed due to high autoclave pressure. Typically, tools used for composites manufacturing are made of isotropic materials including steel, aluminum, and alloys such as INVAR and their CTE values range from 1.6 (INVAR) to 23.6 μm/m°C (aluminum).[3] For anisotropic materials like carbon epoxy composites, the CTE value depends on fiber orientation; composite has less thermal strain in the fiber direction (−0.5 μm/m°C) than in the transverse direction (32.0 μm/m°C).[3] On the other hand, thermoset composites develop cure shrinkage caused by chemical shrinkage of the resin, layup compaction due to autoclave pressure, and thickness reduction due to resin bleeding.

One important source of geometrical distortion is the friction force between tool and part. Because of the tool-part deformation mismatch and the elevated autoclave pressure (around 0.55 MPa), the friction force between tool and part induces residual shear stress that results in part warpage.[2] This defect is caused by the gradient of shear stress from the bottom layer in contact with the tool to the top layer of the composite part. When the autoclave pressure is released, the bottom layer contracts in order to liberate the elastic component of stress induced by the friction force during cure, causing a concave distortion with respect to the bottom layer.[4]

Previous studies have used customized devices to measure friction at pressures and temperatures typical of autoclave conditions.[5–8] Martin et al.[8] proposed a method to characterize the friction resistance of woven carbon fiber/epoxy prepregs for sandwich structures. In their approach, a custom-made device was used to quantify the friction interaction of prepreg/prepreg and prepreg/tool at different temperatures and constant pressure. The authors found that prepregs with high resin content had the lowest friction values and therefore were more prone to cause core crush. Ersoy et al.[4] presented a method to characterize friction-induced shear stress at prepreg/prepreg and prepreg/tool interfaces by continuous pulling of overlapping plies during the ramp-up of the cure cycle of carbon/epoxy unidirectional composites. With this method, the authors identified the

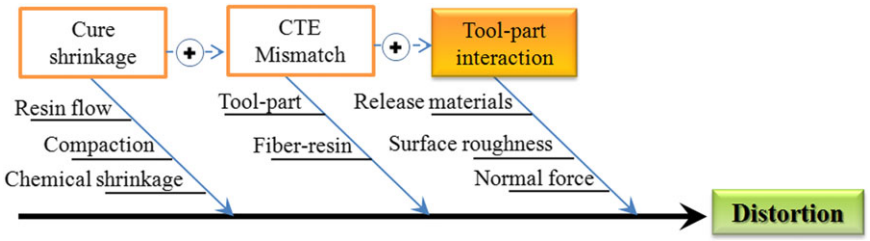

Figure 1. Factors influencing composite part distortion. [Color figure can be viewed in the online issue, which is available at wileyonlinelibrary.com.]

interfacial shear stress during cure and established a gel point-stress relationship. Kaushik and Raghavan[7] measured the static and dynamic coefficient of friction (COF) as a function of degree of cure and implemented a computational model to predict distortion of composite parts. Furthermore, the researchers studied the failure modes at the tool-part interface in which they identified adhesive bonding and cohesive failure of resin.

Twigg et al.[9] presented an alternative method to quantify the shear interaction at the tool-part interface using an instrumented tool with strain gages. The authors used modulated temperature in the cure cycle to study changes in tool thermal strain due to interaction with a composite part. By analyzing the strain readings, the static and sliding frictions were identified since the free thermal expansion of the tool was constrained due to tool-part adhesion when static friction occurred. In a different work, Twigg et al.[10] proposed an analytical model validated by experimental data to predict the maximum part warpage as a function of mechanical properties (modulus of elasticity), geometry (length and thickness), and manufacturing conditions (pressure and tool surface conditions) of composite parts. In their approach, they found that the maximum part warpage was affected by geometry and it was independent of surface conditions when release agent and fluorinated ethylene propylene release film were used.

In composite manufacturing, materials such as fluorocarbon-based release films and polymeric release agents are commonly used to minimize the friction between tools and parts. Because of their rigidity and stability, fluorocarbon-based polymers like PTFE lead to small contact area with most surfaces, reducing the frictional interaction.[11] Researchers have studied the rigidity and microstructure of PTFE films with respect to temperature, showing that change in the film mechanical properties with respect to temperature could vary the frictional interaction between tool and part.[5,12,13] Fote et al.[14] studied the friction behavior of PTFE as a function of temperature and indicated that friction force decreased as temperature increased due to hardness change of polymer.

In another perspective, mathematical models and computational simulations of the tool-part interface are commonly used to predict distortion of composite parts. Because of the complexity of developing mathematical expressions for tool-part contact, researchers have used different alternatives to approximate the interaction between tool and part. Johnston et al.[15] assumed perfect bonding conditions between tool and part to simulate composite distortion. Fernlund et al.[16] implemented in their simulations a shear layer between the tool and the part where the mechanical properties of such layer were changed to mimic a bonded or sliding condition. Zeng and Ragavan[17] used a simplified friction model where the pressure-friction relation was assumed linear. Finally, Kaushik and Raghavan[7] presented computational results where frictional tool-part interaction values were measured experimentally.

In this work, the shear stress between an aluminum tool and a carbon fiber/epoxy composite was investigated during cure using a customized friction rig that applies pressures and temperatures typical of autoclave. The aim was to study the tool-part shear stress as a function of autoclave processing conditions: temperature, surface conditions, pull-out speed (part length), and normal force (autoclave pressure). Furthermore, a mathematical approach to characterize the friction at the tool-part interface was proposed by modifying the Coulomb friction model to account for the aforementioned autoclave processing conditions. Shear stress characterization was developed using two release materials (TFE release film and polymeric release agent) commonly used for composites processing. In addition, the decrease in shear stress caused by different combinations of release materials and surface roughness was investigated, and the contribution of mechanical interlocking to friction was identified. The static/dynamic COF ratio indicating the threshold stress value to initiate sliding between tool and part was measured using three different pull-out speeds. Moreover, the transition between static and dynamic friction was investigated by measuring stress response to modulations of temperature in the cure profile, differing from previous studies[9] where strain gages were used to measure the strain response and characterize the static and dynamic friction at the tool-part interface. The results presented in this article will provide a better understanding of residual stress induced by tool-part interaction during autoclave composites processing.

MATERIALS AND METHODS

Friction Rig

A customized friction rig apparatus was built and used to measure the friction force at the tool-part interface at different temperatures and pressures typical of autoclave. In this apparatus, as shown in Figure 2, a pneumatic piston applies pressure to a prepreg sample placed between two metal plates, and the mobile plate on the fixed rig is then pulled by a universal testing machine (UTM) from MTS. Further details of the friction rig were described by the authors in previous work.[6] According to ASTM

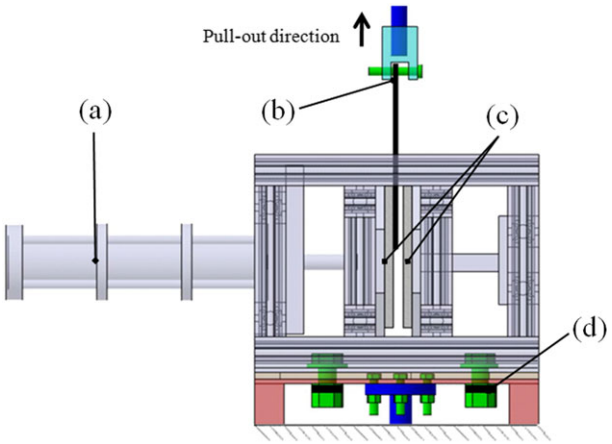

Figure 2. Description of the friction rig: (a) pneumatic piston, (b) mobile plate, (c) metallic plates, (d) elastomeric bushings used for modulated temperature tests. [Color figure can be viewed in the online issue, which is available at wileyonlinelibrary.com.]

G115, the friction rig works as a conforming-surface-tribosystem where the unit of measurement is pull-out force. Figure 3 illustrates an analogy between the friction rig and the autoclave processing in which the force equations corresponding to the friction rig are:

$$\tau = \frac{F}{\mathrm{A}} \qquad (1)$$
$$\mathrm{P} = \frac{F_N}{\mathrm{A}}$$

where τ is the shear stress induced by the tool-part interaction force F, A is the sample area, and P is the pressure generated by the normal force F_N.

Figure 4 shows the principle of part deformation relative to the tool due to CTE mismatch. This principle was used to define the pull-out speed of the friction rig:

$$v = x\frac{\Delta T}{\Delta t}\left(\mathrm{CTE_{tool}} - \mathrm{CTE_{part}}\right) \qquad (2)$$

where v is the speed of the part with respect to the tool at point x, $\mathrm{CTE_{tool}}$ and $\mathrm{CTE_{part}}$ are the CTE of the tool and the part, respectively, and $\Delta T/\Delta t$ is the heat up ramp of the cure cycle.

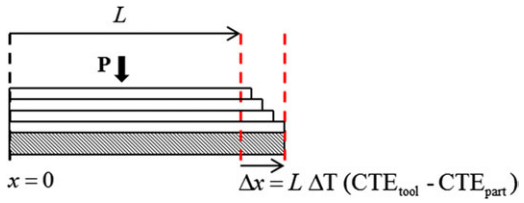

Figure 4. Diagram of displacement caused by CTE mismatch from the center to the edge of the part. The displacement in the center is zero and in the edge is Δx. [Color figure can be viewed in the online issue, which is available at wileyonlinelibrary.com.]

The rate of deformation in both ends of the part could be described by the equation proposed by Ersoy et al.[4] [eq. (3)] in which the shear stress under typical autoclave processing conditions can be measured:

$$v_{\max} = L\frac{\Delta T}{\Delta t}\left(\mathrm{CTE_{tool}} - \mathrm{CTE_{part}}\right) \qquad (3)$$

where L is the half of the total length of the part and v is the crosshead speed of the UTM. The maximum displacement rate ($v_{\max} = 0.07$ mm/min) of the tool with respect to the part was calculated by considering a part with $L = 1$ m, $\mathrm{CTE_{tool}} = 23.6$ μm/m °C (aluminum), $\mathrm{CTE_{part}} = -0.5$ μm/m °C (carbon fiber in the longitudinal direction), and $\Delta T/\Delta t = 2.8$°C/min. Note that in order to simplify the velocity profile in the crosshead of the UTM, the factors such as chemical shrinkage and internal heat generation were not included in eq. (3). Therefore, the friction force was characterized using three different pull-out speeds (0.05, 0.10, and 0.15 mm/min) where $v_{\max}$ was assumed as the reference value. With the aim of studying the dynamic COF, the displacement rate was held constant during the cure cycle and the direction was not changed during cool-down.

Materials

Coupons of 10 × 10 cm^2 of carbon fiber/epoxy unidirectional prepreg (Cytec IM7/977-2) with a stacking sequence $[0°]_2$ were placed on both sides of a stainless steel mobile plate, as shown in Figure 3(a). The width of this plate was the same as the width of the sample coupon to minimize changes in contact area due to resin flow and fiber spreading.

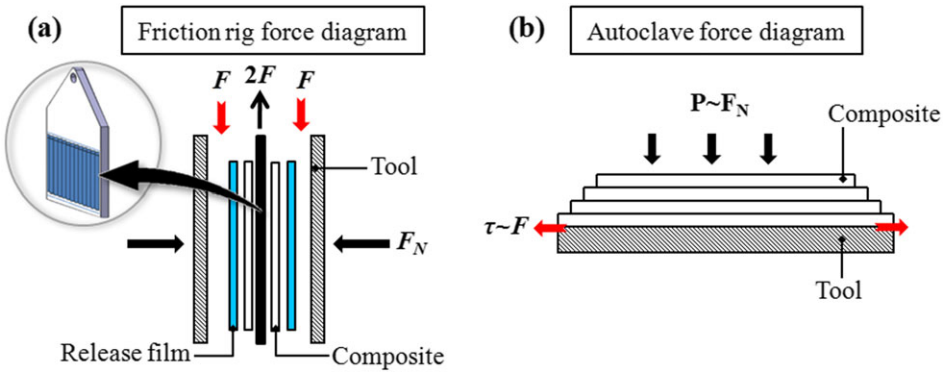

Figure 3. (a) Force diagram of the friction rig and (b) force diagram of autoclave conditions. [Color figure can be viewed in the online issue, which is available at wileyonlinelibrary.com.]

Table I. Set of Experiments Used to Characterize Shear Stress

Analysis	Test	Experiments	Results (Figure)
Method 1[a]	During cure cycle	6	5
	Cool-down region	6	6
	Cured sample and release film	1	7
	Modulated temperature		
	With modulation	2	10
	Without modulation	2	10
	Shear stress vs. pressure	5	14
Method 2[b]	During cure cycle	6	8
	Modulated temperature		
	With modulation	2	11
	Without modulation	2	11
	Shear stress vs. pressure	5	14
Surface roughness	1.35 μm (120 grit sand paper)	1	12
	0.18 μm (400 grit sand paper)	1	12
	0.18 μm and release agent	1	12
Rheology	Rheological analysis	1	9

[a]Method 1: TFE release film in addition to release agent.
[b]Method 2: Release agent only.

The tools of the friction rig [Figure 3(a)] were made of aluminum 6061. Tool surfaces were conditioned with a 400 grit sand paper and cleaned with solvent before testing. The surface roughness was measured using a surface roughness tester (Mitutoyo SJ-201) and the root-mean-squared surface roughness value (R_q) obtained for both tools was 0.18 μm, which corresponds to the typical surface conditions found in industrial applications.[18] Tools were treated with mold sealer (Frekote B-15) and then cured inside an oven for 1 h at 94°C. Two release methods were used on the surface of the tool: method 1 consisted of placing a tetrafluoroethylene (TFE) release film (Airtech WL-5200 blue) in addition to release agent (Frekote 770NC), while method 2 consisted of using only release agent.

Test Parameters

Shear stress characterization tests were performed at a pressure of 0.55 MPa (80 psi) following the manufacturing recommended cure cycle. Samples were cured at a ramp rate of 2.7°C/min until 177°C and then held at this temperature for 3 h.

To study the stress-temperature behavior and the transition point between static and dynamic shear stress, temperature modulations were incorporated in the cure cycle. An amplitude of ±2°C, which is of the same order of magnitude as that used by Twigg et al.,[9] was generated using a LabVIEW interface and an adaptive PID controller for the heating hardware of the friction rig. To perform the modulated temperature tests, the friction rig was modified to a high deformation configuration by placing elastomeric bushings on the bolts that connect the friction rig to the UTM base (Figure 2). This configuration increased the sensitivity of the friction rig allowing for a clear distinction between static and dynamic friction. Note that this configuration was used only with modulated temperature tests, since the high deformation configuration of the rig may result in tool-part displacements that do not correspond to the crosshead displacement of the UTM.

The effect of pressure on shear stress was investigated by testing samples subjected to pressures between 0.27 MPa (40 psi) and 0.83 MPa (120 psi) during the cure cycle without modulating temperature. Table I describes the experiments performed in this investigation.

Rheological Analysis

A rheological analysis was performed using a rheometer ATD 2000 ESR (AvPro, Alpha Technologies) to correlate the shear behavior with the viscoelastic properties of the composite. This method encapsulates the sample (stacking sequence $[0^\circ]_{28}$) between parallel plates and applies shear stress during cure. The nonmodulated temperature profile of the friction rig was imported into the rheometer in order to set the cure profile for the tests. ASTM D4473 was followed to analyze the obtained data.

RESULTS AND DISCUSSION

Stress Analysis for Samples Tested with Release Film

Figure 5 depicts changes in shear stress at different pull-out speeds during cure of samples containing release film and release agent (method 1) between tool and part. Figure 5(a) shows transitions in shear stress with respect to time while Figure 5(b) shows changes in shear stress relative to temperature. As indicated in Figure 5(b), the change in shear stress in the A–C region was initially associated with an increase in resin flow velocity[19] until ~ 70°C and a subsequent increase in stress due to development of mechanical properties of the resin during cure until point C. After point C [Figure 5(a)], the shear stress reached a plateau value until cooling (D) where the stress began to increase while decreasing temperature. Note that point C corresponds to the gel point of the resin, as it will be explained in Rheological Analysis section.

Figure 6 shows the change in shear stress with respect to temperature during the D–E region. The stress-temperature relations were approximated to linear trends and the minimum R^2 value obtained was 0.99. Notice that stress was plotted in linear scale. The slopes of the trend lines showed a stress-temperature dependence between -0.3×10^{-3} and -0.8×10^{-3} MPa/°C. These results could describe the interaction between release materials and tool since the composite has a degree of cure close to 1. To prove this assumption, the shear stress corresponding to the release materials was measured using a fully cured sample. The film was wrapped through the slot of the mobile plate in order to prevent displacement between film and composite, as shown in Figure 7(a). An experiment was then carried out at 0.10 mm/min following the temperature profile shown in Figure 5(a). Results shown in Figure 7(b) indicated that slopes for heating up and cooling down (-0.3×10^{-3} and -0.4×10^{-3} MPa/°C) were in the same order of magnitude as

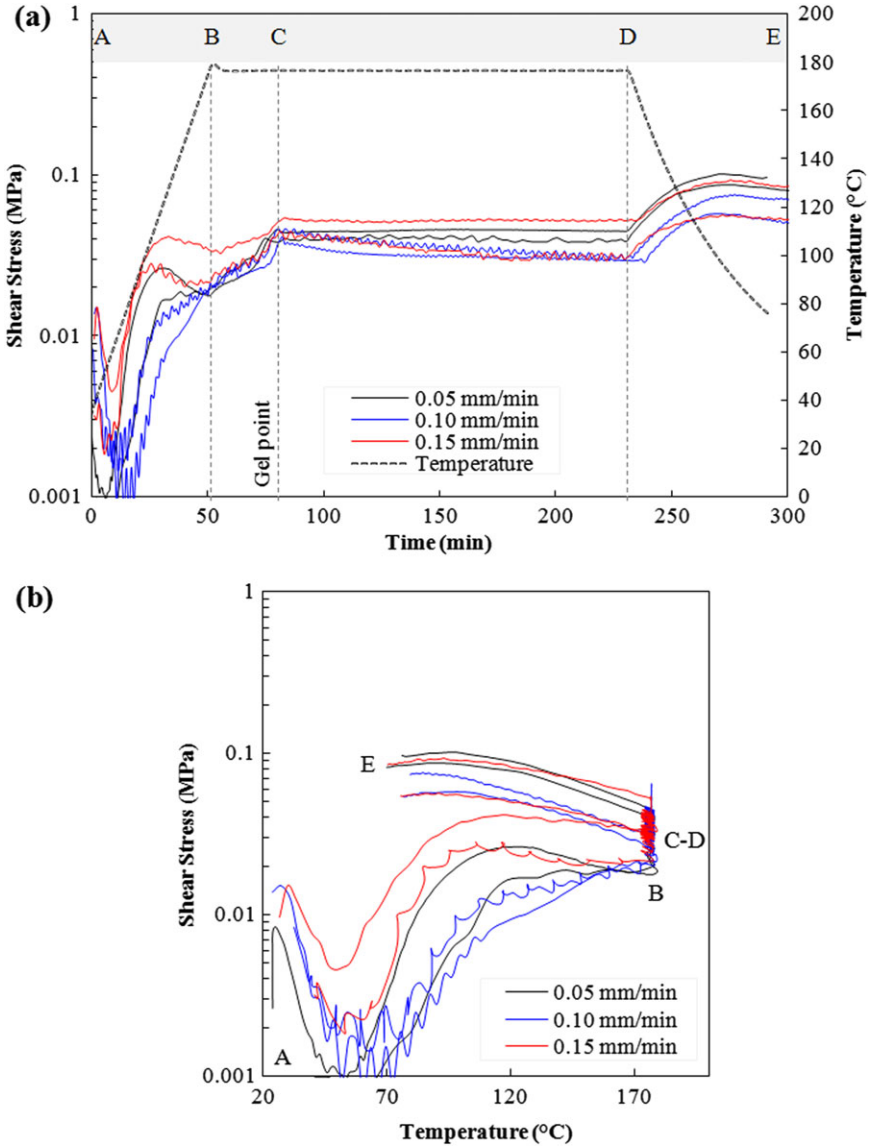

Figure 5. (a) Stress-time and (b) stress-temperature behavior at different pull-out speeds (0.05, 0.10, and 0.15 mm/min) using release film (method 1). The cure cycle stages are: heat up (region A–B), dwell (region B–C–D), and cool-down (region D–E). [Color figure can be viewed in the online issue, which is available at wileyonlinelibrary.com.]

the slopes of the trend lines presented in Figure 6. These results showed that frictional stress during cooling (D–E region) was governed by the release material. In addition, they highlight the tool-part shear stress dependency on temperature.

Shear Stress Behavior Using Release Agent

The shear stress results of samples tested with polymeric release agent (method 2) are shown in Figure 8. In this figure, tests performed at 0.10 and 0.15 mm/min depicted ~ 24% higher stress values in the C–D region than those corresponding to release film [Figure 5(a)]. Furthermore, samples tested at 0.05 mm/min showed a shear stress of more than 0.2 MPa indicating strong adhesion between the composite coupon and tool. The sudden stress decrease after 150 min indicated adhesion failure resulting in a subsequent stress behavior similar to that shown by the samples tested at 0.10 and 0.15 mm/min. Since, pull-out rates of 0.05 mm/min represent composite parts of 0.07 m in length [as indicated by eq. (3)], results imply that parts smaller than 0.07 m are likely to remain adhered on the tool when release agent is used. On the other hand, a strong adhesion was not noticed in samples tested above 0.05 mm/min or when using release film [Figure 5(a)] because smaller stress peaks after point C were measured. On the basis of these results, it is concluded that parts processed with release agent (method 2) might develop higher geometrical distortion than parts where release film (method 1) is used at the tool-part interface.

Note also that analysis of stress-temperature dependence in the D–E region showed values between -0.3×10^{-3} and -0.4×10^{-3} MPa/°C with an $R^2 \leq 0.97$ [Figure 8(b)], meaning that shear stress was less sensitive to temperature when tests were performed with release agent (method 2).

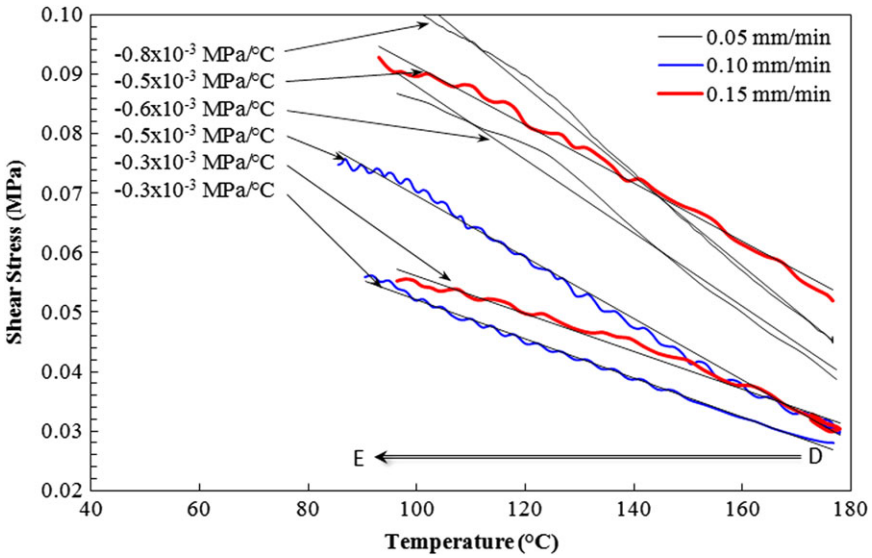

Figure 6. Variation of shear stress at different speeds with respect to temperature during cool-down (region D–E). [Color figure can be viewed in the online issue, which is available at wileyonlinelibrary.com.]

Rheological Analysis

Figure 9 shows changes in shear modulus of the composite material during the cure cycle. According to ASTM D4473, the gel point is defined as the maximum value of Tan(δ). In agreement with the results presented by Alavi-Soltani et al.,[20] gelation of the prepreg IM7/977-2 UD occurred at the 74th min, which corresponded to point C showed in previous results. Therefore, point C related the gel point to the starting point of the shear stress plateau when release film was used [Figure 5(a)]. For release agent, on the other hand, the gel point was identified at the beginning of the stress peaks [Figure 8(a)].

The minimum shear stress shown in Figures 5 and 8 was measured around the 20th min (70°C in A, B region), which corresponded to the maximum resin flow velocity of IM7/977-2UD reported by Ahmed.[19] In addition, the minimum viscosity of this particular prepreg was identified in Figure 9 around the 45th min of the cure cycle, in agreement with the literature.[21] The discrepancy between the point of maximum resin flow velocity and minimum viscosity can be associated with the interaction of the fiber bed. As described by Dave et al.,[22] the fibers without resin behave as porous solids, which exert a reaction force (spring-like behavior) when subjected to autoclave pressure. Accordingly, the authors described that the autoclave pressure gradually transfers from the resin to the fiber bed while the resin bleeds in a process that they defined as sequential compaction. Thus, the resin flow velocity might decrease before reaching the point of minimum viscosity due to a reduction in resin pressure. On the basis of these findings, it is suggested that the results of minimum shear stress (20th min) during cure were related to the maximum resin flow velocity and not to the minimum viscosity point.

Modulated Temperature Test

Shear stress response with respect to temperature was investigated by modulating the temperature during the cure cycle, as mentioned in section Test parameters. This methodology was

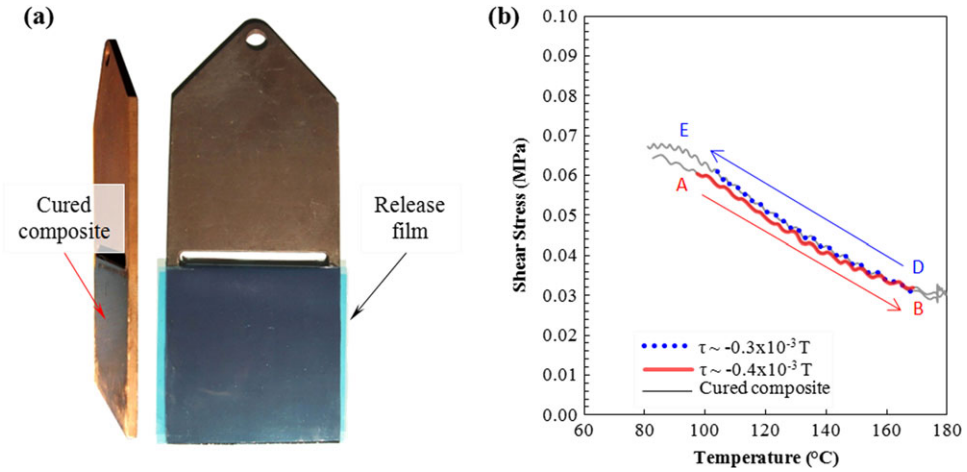

Figure 7. (a) Release film set-up on the mobile plate and (b) stress as a function of temperature for release film. [Color figure can be viewed in the online issue, which is available at wileyonlinelibrary.com.]

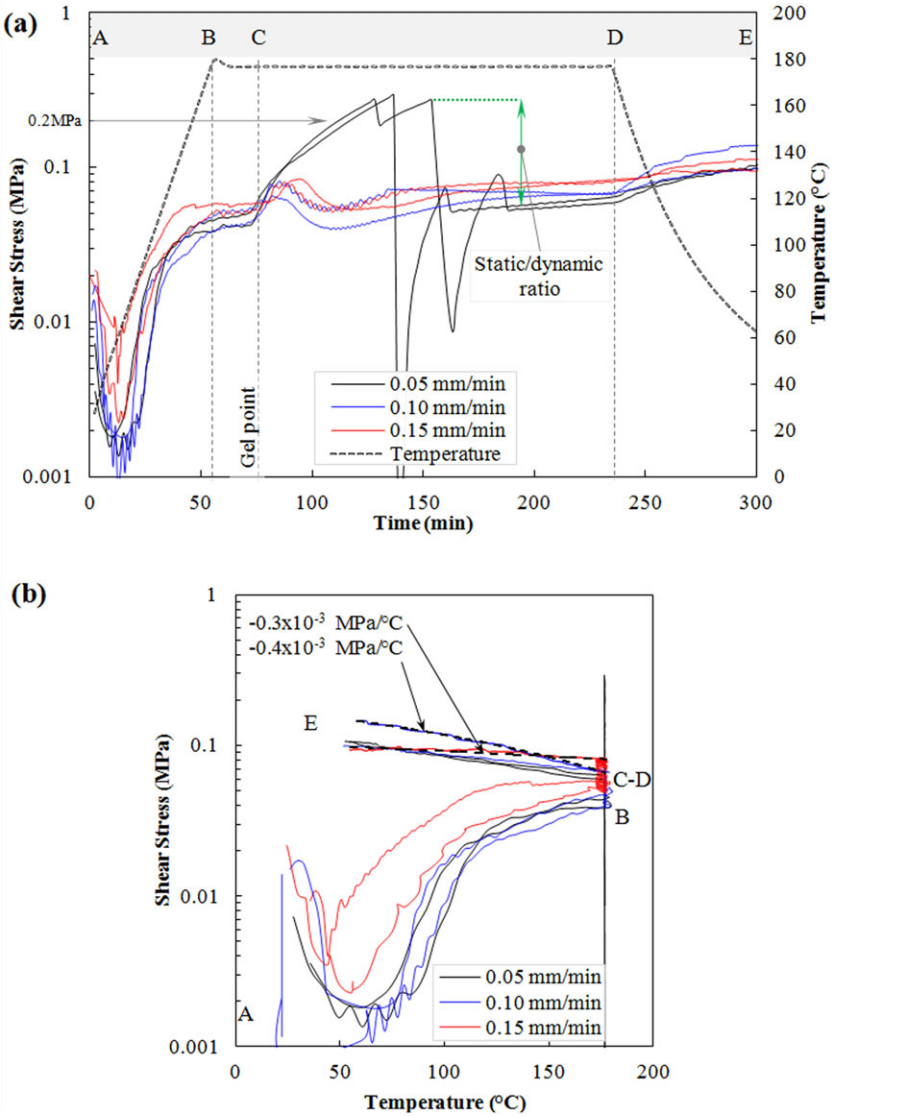

Figure 8. (a) Stress-time and (b) stress-temperature behavior using release agent (method 2). [Color figure can be viewed in the online issue, which is available at wileyonlinelibrary.com.]

used to establish the conditions in which shear stress depended on temperature (as observed in Figure 6) for each combination of release materials. Note that the friction rig was modified to a high deformation configuration with the aim of improving stress sensitivity to temperature, and the experiments, summarized in Table I, were carried out at 0.05 mm/min.

The shear stress behavior with and without temperature modulations was compared in Figure 10 for release film (method 1), and Figure 11 for release agent (method 2). Modulated tests for release film depicted remarkable stress oscillations after 120 min while, for release agent, slight stress oscillations were shown after the breakaway point of the sample with the lowest stress value. These results imply that the stress response to temperature fluctuations could be used to identify the dynamic frictional stress because the shear stress was dependent on temperature only when the part was moving with respect to the tool. As such, the static/dynamic stress ratio was calculated with the maximum shear stress value divided by the plateau stress (as indicated in Figure 10), and the results corresponding to this stress ratio are shown in section "Effect of pull-out speed on shear stress".

Modulated temperature profiles also showed to be effective in reducing static frictional interactions between tool and part. Initially, nonmodulated tests showed clear breakaway points around the 145th min of Figure 10, but these points were not noticed in modulated tests. The absence of breakaway points indicated that temperature modulations caused strain oscillations at the tool-part interface that induced the dynamic friction. This effect was also evident in Figure 11 where modulated tests showed breakaway stress values 2.43 ± 0.13 times lower than nonmodulated tests and a reduction of tool-part interface stress at ~ 200 min. Note that these samples presented two breakaway points corresponding to sample failure on each sides of the mobile plate. Therefore, temperature modulated profiles

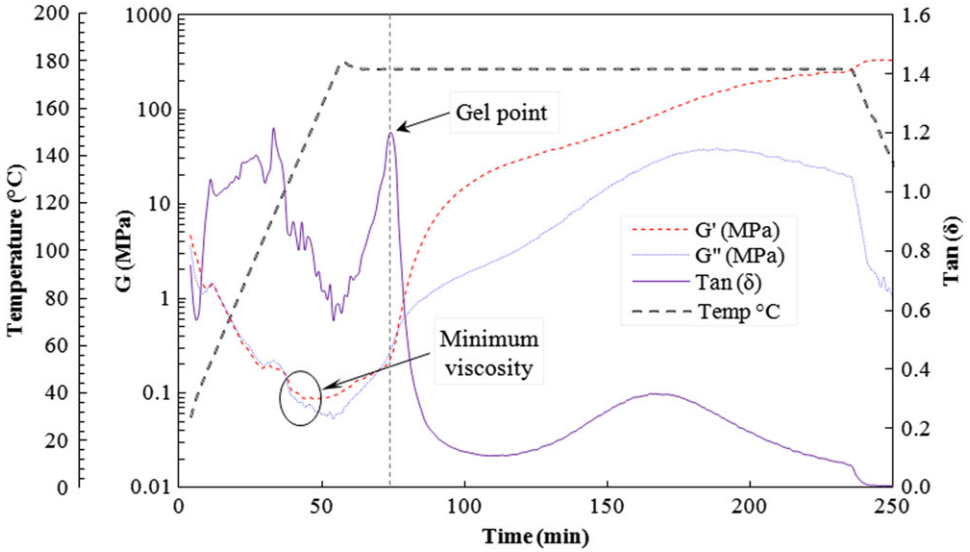

Figure 9. Rheological characterization of the prepreg IM7/977-2 UD. [Color figure can be viewed in the online issue, which is available at wileyonlinelibrary.com.]

can be used as an alternative methodology to reduce the peak in static frictional stress.

Effect of Pull-Out Speed on Shear Stress

Experiments indicated that static COF depended on pull-out speed when using release agent. Tests performed at 0.05 mm/min [Figure 8(a)] showed a static/dynamic friction ratio of 5.29 ± 0.19, which indicated tool-part adhesion. In contrast, tests performed at speeds higher than 0.05 mm/min [Figure 8(a)] showed lower static/dynamic stress ratio (1.6 ± 0.1), which seemed to be associated with a weaker interaction between tool and part. Hence, parts shorter than 0.7 m in length, which corresponds to a pull-out speed of 0.05 mm/min [eq. (3)], would present adhesion at the tool-part interface, while longer parts might not present adhesive behavior. On the contrary, test performed with release film did not show any speed dependence on shear stress and the static/dynamic stress ratio was between 1 and 1.1.

The dynamic COF and the shear stress after the breakaway points did not show a strong dependence on pull-out speed. Experiments performed at different speeds (0.05–0.15 mm/min) did not affect the shear stress for both release methods (Figures 5 and 8). These results agreed with the findings observed by Biswas and Vijayan in which the COF of fluoropolymers was independent of speed for values below 60 mm/min.[13]

Effect of Tool Surface Conditions on Shear Stress

The contribution of mechanical interlocking on shear stress was characterized by performing two tests with different surface conditions. Tool surfaces were modified using sand papers of 400 and 120 grit and their resultant surface finish were 0.18 and

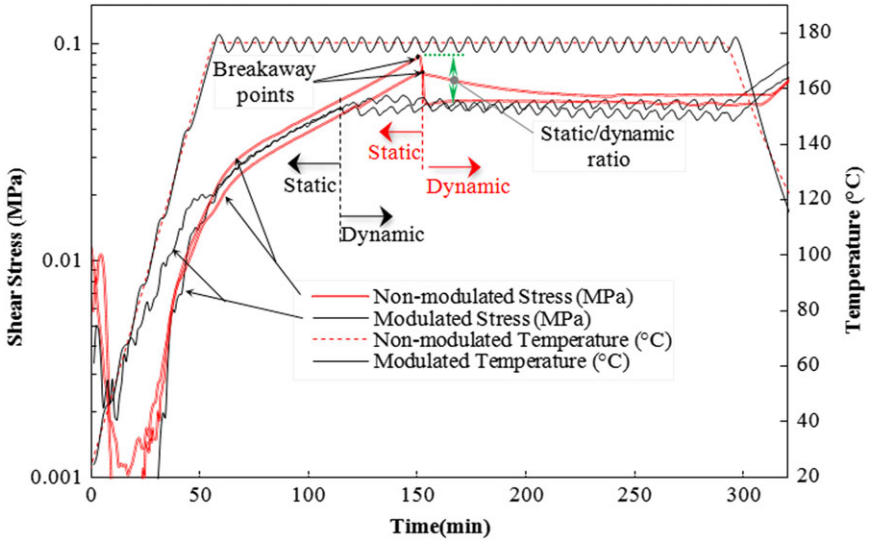

Figure 10. Modulated temperature test for release film. [Color figure can be viewed in the online issue, which is available at wileyonlinelibrary.com.]

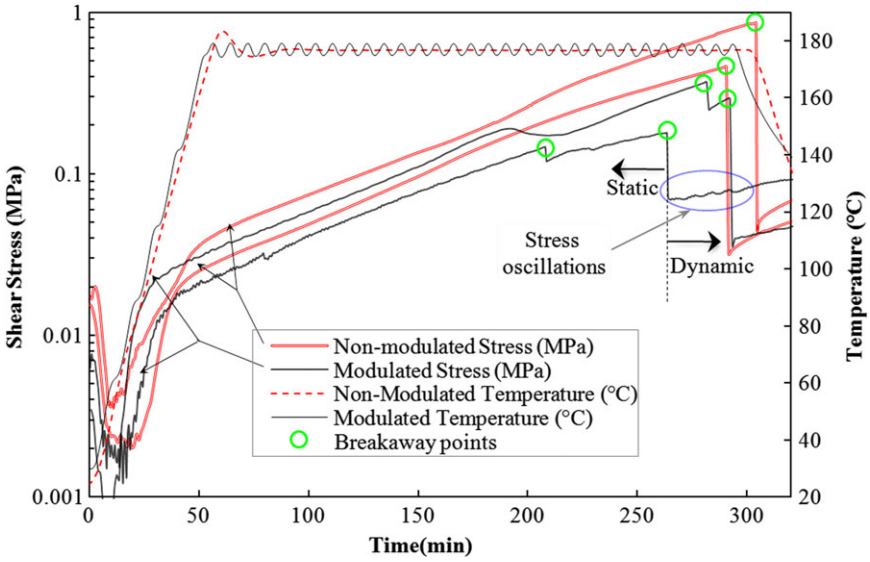

Figure 11. Modulated temperature test for release agent. [Color figure can be viewed in the online issue, which is available at wileyonlinelibrary.com.]

1.35 μm, respectively. Tests performed only with release film (not with release agent) showed a 10–27% decrease in shear stress when tool roughness was reduced by 1.17 μm (Figure 12). To study the release agent contribution on shear stress, a third sample was prepared following method 1 and tested using a tool with a surface roughness of 0.18 μm. Results showed a decrease in shear stress between 23% and 51% when applying release agent. Note that the variance in shear stress decrease is associated with the different stress-temperature slopes for each tool surface condition or release material, which can be explained by the interaction mechanisms described by Bowden and Tabor.[11] The authors presented results suggesting that fluorocarbon based polymers (release materials) have two main contributors related to material hardness and surface energy (mechanical and thermodynamic interactions, respectively). As such, it is valid to assume that mechanical interactions between tool and part in the presence of a release material are associated with surface roughness while thermodynamic interactions are caused by the effect of the release agent on the release film. As observed in Figure 12, the predominance of thermodynamic interaction over mechanical interlocking was observed by a stress reduction of up to 51% when using release agent.

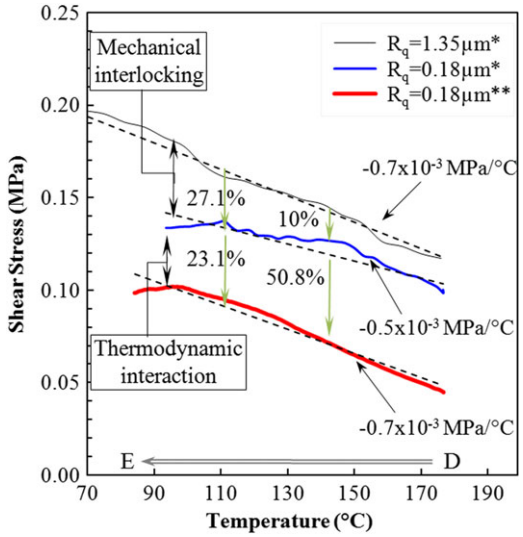

Figure 12. Effect of surface conditions on the stress-temperature relation during cool-down (D–E region). Test speed: 0.05 mm/min. *Release film without release agent. **Release film with release agent. [Color figure can be viewed in the online issue, which is available at wileyonlinelibrary.com.]

In conclusion, composite parts manufacturers should find the most appropriate combination of release materials for their application rather than minimize the frictional interaction by mechanical sanding that could translate into higher manufacturing costs.

Temperature–Friction Relation

Modulated temperature results (section "Modulated Temperature Test") indicated that shear stress depended only on temperature when the part was moving with respect to the tool. In addition, the results corresponding to tool surface condition (section "Effect of Tool Surface Conditions on Shear Stress") showed that tool-part interaction comprised both mechanical and thermodynamic interactions, which decreased linearly with temperature (Figure 12). From the mechanical interlocking point of view, the decrease of COF with respect to temperature could be approximated to a linear function based on the reduction in hardness of the PTFE.[12,1,4] On the other hand, fluorocarbon-based polymers exert low thermodynamic interaction with the counter surfaces due to low surface energy[11] that decreases linearly as a function of temperature.[23] As such, the dynamic friction behavior could be approximated by a linear function of temperature, and an expression could be formulated to describe the shear stress-temperature relation based on the physics of the friction behavior and the experiments [eq. (4)]:

$$\tau = k(cT_c - T) \quad (4)$$

Applied Polymer SCIENCE

Table II. Constant Used to Calculate the Kinetic COF (μ_k)

Release system	*a*	*b*
Release film	$-0.95 \times 10^{-3} \pm 0.35 \times 10^{-3}$	0.245± 0.08
Release agent	$-0.60 \times 10^{-3} \pm 0.1 \times 10^{-3}$	0.20.7 ± 0.02

where τ is the shear stress under dynamic conditions, and T is temperature. T_c, k, and c are assumed as constants in order to maintain a linear relation between shear stress and temperature. T_c is a hypothetical critical temperature at which the polymer begins to degrade or melt.[23] Substituting eq. (4) in the classical definition of COF [eq. (5)], the kinetic COF (μ_k) can be calculated as shown in eq. (6).

$$\mu = \frac{F_f}{F_N} = \frac{\tau}{\mathrm{P}} \tag{5}$$

$$\mu_k(T) = a\,T + b \tag{6}$$

where a, b, are constants. Because the study of c, k, and T_c is beyond the scope of this work, results were focused on the parameters of eq. (6), which are sufficient to establish a relation between frictional force and temperature. The parameters a and b (shown in Table II) were calculated directly from the experimental results, and the predicted COF [eq. (6)] was compared with the samples that showed the maximum and minimum stresses in the C, D region (normalized with respect to pressure), as shown in Figure 13.

The parameter a was calculated by dividing the value of the stress-temperature slope in the D–E region [Figures 6 and 8(b)] by the friction rig pressure (0.55 MPa), as indicated in eq. (5). In section "Stress analysis for samples tested with release film", it was shown that during the D–E region the shear stress was governed mainly by the behavior of the release material at the tool-part interface. Since, results of Figure 7(b) showed that the release materials were stable during the cure cycle of the composite, the COF measured in the D–E region can be used to determine the COF in any other region. Figure 13 proves this assumption since the shear stress measured in the A–C region did not exceed the predicted COF for the reason that the composite coupons remained adhered to the tool until the threshold value equivalent to the static stress was reached. In the vicinity of point C, the threshold stress was reached and results indicated that samples began to slide on the tool since a plateau in stress was measured (dynamic friction). Therefore, the parameter a represents the rate of change of COF with respect to temperature during the A–B and D–E regions.

The fitting factor b was calculated from the range of stresses measured at the beginning of the C–D region (dynamic shear stress) of Figure 13 neglecting wear and abrasion effects at the tool-part interface. During this region, the measured COF showed a deviation from the predicted COF due to abrasion mechanisms. In the release agent case, the difference between measured and predicted COF were possibly associated with wear in the counterfaces.[24] Further, a slightly negative slope was identified for release film [Figure 13(b)], which could be related to polymer deposition on the tool as a result of abrasive effects on the surface.[25] Similar effects could explain the differences observed during D–E region. However, in eq. (6) abrasion was not included because the tool-part displacement rate diminishes as the degree of cure of the composite advances.

Finally, the values of COF depicted in Figure 13 were compared with those found in the literature. Dynamic COF values of 0.07 ± 0.02 at 177°C (point C) and 0.21 ± 0.07 at room temperature (point E) were calculated using release film [eq. (6)]. On the other hand, values of 0.1 ± 0.005 at 177°C and 0.20 ± 0.02 at point E were calculated for release agent. These values were lower than the COF results (around 0.3–0.6) reported in the literature[24] for carbon fiber composites tested with a metallic counter surface measured at room temperature due to the use of release materials.

Effect of Pressure on Shear Stress

Figure 14 shows the values of dynamic shear stress at different pressures when release film (method 1) and release agent (method 2) were used. Results showed a linear variation of

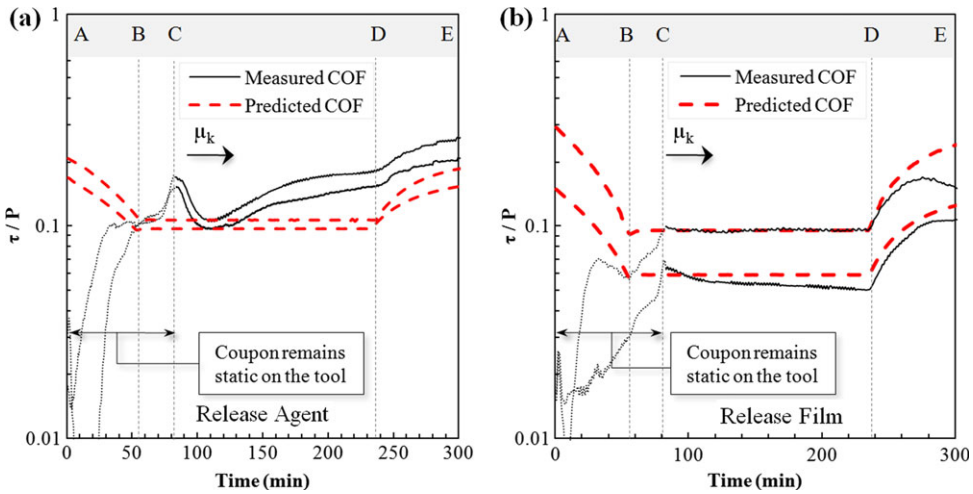

Figure 13. Measured and predicted COF during cure for release film and release agent. [Color figure can be viewed in the online issue, which is available at wileyonlinelibrary.com.]

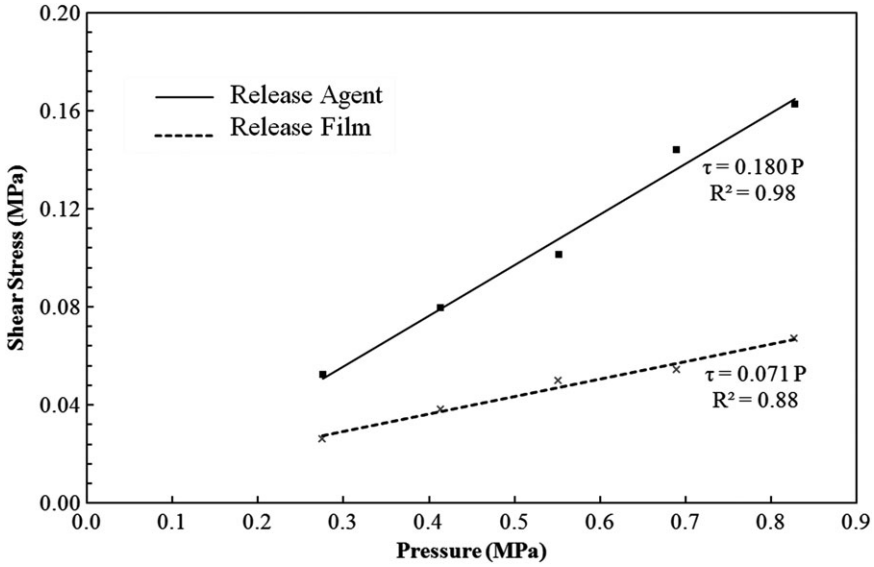

Figure 14. Shear stress (plateau C–D) as a function of pressure for release film and release agent.

shear stress with respect to pressure for both methods. These results agreed with the classical definition of COF, eq. (5), where it was indicated that normal and frictional forces could be directly proportional.

In the literature was mentioned that although polymers might have a linear dependence on normal force, these materials commonly depict nonlinear trends.[7,11] For this reason, Bowden and Tabor[11] suggested a model based on experimental data:

$$F_f(P) = \mathrm{k}_1 \, (F_N)^{k_2} \tag{7}$$

where $k_2 \leq 1$ for polymers. This model can be used to analyze the results obtained in Figure 14, which indicate that for this particular case values of k_1 and k_2 were approximately μ and 1, respectively.

Mathematical Approach to Determine Friction Force

A mathematical approach was proposed to predict the frictional interaction between tool and part as a function of the principal variables corresponding to autoclave processing conditions. By modifying the Coulomb friction model to account for temperature variation [eq. (8)], a mathematical approach was proposed to calculate the friction force at the tool-part interface, as shown in eq. (9).

$$F_f(P,T,t) = -F_N(P) \; \mu_k(T) \; \mathrm{sign}(v(t)) \tag{8}$$

In this model, the normal force F_N was calculated from eq. (5) and the kinetic COF $[\mu_k(T)]$ was determined from eq. (6). The term sign $(v(t))$ represented the direction of speed associated with the relative movement of the part due to deformation mismatch.

$$F_f(P,T,t) = -\frac{P}{\mathrm{A}} \; (\mathrm{a}T + \mathrm{b}) \; \mathrm{sign}(v(t)) \tag{9}$$

This mathematical approach was complemented with the results corresponding to the transition between static and dynamic friction. The static-dynamic COF ratio (μ_s/μ_k) for parts shorter than 0.07 m in length was 5.29 ± 0.19 and for longer parts was 1.6 ± 0.1 when using release agent. In contrast, the ratio μ_s/μ_k was 1-1.1 regardless of the part length (pull-out speed) when using release film.

The significance of eq. (9) can be explained by the deformation mismatch between tool and part. As observed in Figure 4, the tool-part deformation mismatch is zero in the center of the part and increases toward the edges during the cure cycle. Twigg et al. described the transition between static and dynamic friction as a point (debond front) that migrates from the edges toward the center of the part as tool-part deformation mismatch developed during cure.[9] In this context, the normal force (autoclave pressure) and the tool-part friction interaction induce a gradient of stress along the part. For small deformations and stresses lower than the maximum static shear stress, eq. (10a), the part remains static with respect to the tool. For large deformations, the shear stress surpasses the static COF (μ_s) and it reaches a constant value corresponding to the kinetic COF (μ_k), as shown in eq. (10b).

$$\tau \leq \mu_s P \tag{10a}$$

$$\tau_k = \mu_k P \tag{10b}$$

Future work would be oriented toward the implementation of this model using numerical methods to predict distortion of composite laminates.

CONCLUSIONS

The friction interaction between a composite part and an aluminum tool was characterized using temperatures and pressures typical of autoclave processing. The effects of pull-out speed (part length), temperature, tool surface condition, and normal force (autoclave pressure) on the friction force were investigated. To predict the COF as a function of these variables, a

modified approach comprising the Coulomb's friction model was proposed for two release materials: release film and release agent.

Samples tested using the release film showed lower static and dynamic COF than samples tested using the release agent. Results using the release film depicted values of dynamic COF between 0.05 and 0.09 at 177°C, while this COF increased to 0.09–0.11 when using the release agent. Additionally, the static/dynamic COF ratio was measured to be between 1 and 1.1 for the release film, indicating a weak tool-part interaction. For the release agent, the COF ratio depended on the pull-out speed. The ratio increased to 5.29 ± 0.19 at pull-out speed of 0.05 mm/min, while it was 1.6 ± 0.1 at higher speeds, which implies tool-part adhesion for parts shorter than 0.7 m (0.05 mm/min). In general, results indicated that parts processed with the release film had lower tool-part interaction than those where the release agent was used. Consequently, lower geometrical distortion might result using the release film.

Similarly, samples tested at pressures between 0.27 MPa (40 psi) and 0.83 MPa (120 psi) showed lower dynamic shear stress values using the release film. For both release materials, tests also showed a linear stress-pressure relationship, which was in agreement with the classical definition of friction.

Experiments indicated that dynamic shear stress showed significant dependence on temperature, which is not included in the classical definition of friction force. A change with respect to temperature from 0.3×10^{-3} to 0.8×10^{-3} MPa/°C was measured for the release film and from 0.3×10^{-3} to 0.4×10^{-3} MPa/°C for the release agent. Moreover, modulated temperature analyses indicated that the release film had higher shear stress response to temperature variations. On the basis of these results, a new approach based on the Coulomb's friction model was suggested by including a temperature dependence on the dynamic COF.

Finally, the dependency of COF on mechanical interaction and thermodynamic interactions was investigated. The effect of mechanical interlocking was observed when the shear stress decreased between 10 and 28% due to a change in tool surface roughness (86% smoother). In addition, a decrease up to 51% in shear stress for samples tested with the release agent was measured in comparison to samples with the release film only, which indicated a thermodynamic interaction between the tool and the part. On the basis of these results, it was concluded that thermodynamic interactions showed stronger contribution to friction than mechanical interlocking.

ACKNOWLEDGMENTS

The authors gratefully acknowledge financial support from the National Aeronautics and Space Administration (Grant No. NNX09AO58A).

REFERENCES

1. Huang, X.; Gillespie, J. W.; Bogetti, T. *Compos. Struct.* **2000**, *49*, 303.
2. White, S. R.; Hahn, H. T. *J. Compos. Mater.* **1992**, *26*, 2423.
3. Callister, W. D. Materials Science and Engineering: An Introduction; Wiley: New York;**2007**.
4. Ersoy, N.; Potter, K.; Wisnom, M. R.; Clegg, M. J. *Compos. A: Appl. Sci. Manufact.* **2005**, *36*, 1536.
5. Flanagan, R. PhD thesis, Queen's University of Belfast (**1998**).
6. Joven, R.; Tavakol, B.; Rodriguez, A.; Minaie, B. SAMPE 2010 Conference and Exhibition "New Materials and Processes for a New Economy", May 17, 2010–May 20, 2010, Seattle, WA, United states, 2010, pp Seattle and Eastern Canada SAMPE Chapters.
7. Kaushik, V.; Raghavan, J. *Compos. A: Appl. Sci. Manufact.* **2010**, *41*, 1210.
8. Martin, C. J.; Seferis, J. C.; Wilhelm, M. A. *Compos. A: Appl. Sci. Manufact.* **1996**, *27*, 943.
9. Twigg, G.; Poursartip, A.; Fernlund, G. *Compos. Sci. Technol.* **2003**, *63*, 1985.
10. Twigg, G.; Poursartip, A.; Fernlund, G. *Compos. A: Appl. Sci. Manufact.* **2004**, *35*, 121.
11. Bowden, F. P.; Tabor, D. The friction and lubrication of solids, Part XIII: The friction deformation of polymeric materials; Oxford University Press: Oxford, **1964**.
12. Rae, P. J.; Brown, E. N. *Polymer* **2005**, *46*, 8128.
13. Biswas, S. K.; Vijayan, K. *Wear* **1992**, *158*, 193.
14. Fote, A. A.; Wildvank, A. H.; Slade, R. A. *Wear* **1978**, *47*, 255.
15. Johnston, A.; Vaziri, R.; Poursartip, A. *J. Compos. Mater.* **2001**, *35*, 1435.
16. Fernlund, G.; Rahman, N.; Courdji, R.; Bresslauer, M.; Poursartip, A.; Willden, K.; Nelson, K. *Compos. A: Appl. Sci. Manufact.* **2002**, *33*, 341.
17. Zeng, X.; Raghavan, J. *J. Compos. A: Appl. Sci. Manufact.* **2010**, *41*, 1174.
18. Sloan, J. In: Composites Technology. **2011**. p. 24–29.
19. Ahmed, A.; Wichita State University, Wichita, KS: **2012**.
20. Alavi-Soltani, S.; Sabzevari, S.; Koushyar, H.; Minaie, B. *J. Compos. Mater.* **2012**, *46*, 575.
21. Alavi-Soltani, S. In Mechanical Engineering; Wichita State University: Wichita, KS, **2010**.
22. Dave, R.; Kardos, J. L.; Dudukovic, M. P. *Polym. Compos.* **1987**, *8*, 29.
23. Eötvös, R. *Annalen. der Physik.* **1886**, *263*, 448.
24. Schön, J. *Tribol. Int.* **2004**, *37*, 395.
25. Yang, E. L.; Hirvonen, J. P.; Toivanen, R. O. *Wear* **1991**, *146*, 367.